Intermittently Closed and Open Lakes and/or Lagoons (ICOLLs) as groundwater-dominated coastal systems: Evidence from seasonal radon observations

Mahmood Sadat-Noori[1,2*], Isaac R. Santos[1,2], Douglas R. Tait[1,2], Ashly McMahon[1,2], Sean Kadel[3], Damien T. Maher[2]

[1]National Marine Science Centre, Southern Cross University, Coffs Harbour, New South Wales, Australia

[2]School of Environment, Science and Engineering, Southern Cross University, Lismore, New South Wales, Australia

[3]Queensland Bulk Water Supply Authority (Seqwater), Queensland, Australia

[*]Corresponding author:

M. Sadat-Noori, School of Environment, Science and Engineering, Southern Cross University, PO Box 157, Lismore, NSW 2480, Australia (m.sadatnoori@yahoo.com)

Abstract

Intermittently Closed and Open Lakes or Lagoons (ICOLLs) are dynamic coastal systems that may be vulnerable to changes in catchment hydrology. However, little is known regarding the role of groundwater on the hydrological cycles of ICOLLs. Groundwater discharge in two ICOLLs (Welsby and Mermaid) and a nearby wetland (South Welsby Lagoon) located on Bribie Island (Australia) was quantified using radon (^{222}Rn, a natural geochemical groundwater tracer) from observations made during four seasonal surveys. The distribution of radon revealed temporal and spatial changes over the study period with higher surface water radon concentrations found in winter for Welsby ICOLL and in autumn for Mermaid ICOLL. The average estimated groundwater discharge rates from a radon mass balance were 3.4±2.1, 7.3±8.9 and 2.6±1.1 cm d^{-1} in Welsby, South Welsby and Mermaid Lagoons, respectively. These values are at least 8-fold greater than the average annual precipitation that falls directly over the ICOLLs (1420 mm per year, or 0.4 cm d^{-1}), which, coupled with minimal surface water runoff due to the permeable sandy soils, demonstrates that these systems are groundwater-dominated. Overall, groundwater discharge rates in these ICOLLs was much larger than has been reported in other lake systems which is most likely due to the high permeability of regional sandy soils and their large shoreline to volume ratio.

KEYWORDS: Submarine groundwater discharge, groundwater hydrology, permeable sediments, coastal lagoon, sand island, coastal wetland.

1. Introduction

Intermittently Closed and Open Lakes and Lagoons (ICOLLs) are brackish coastal water bodies with a connection to the ocean that is closed periodically due to the accumulation of marine sediment forming an entrance berm (Haines, 2006). Such systems may also be referred to as semi-permanently closed estuaries, temporarily open-closed estuaries, or simply, coastal lagoons in different parts of the world (Haines et al., 2006). ICOLLs are characterised by intermittent surface water inflows and the opening of ICOLLs usually occurs shortly after periods of high rainfall. ICOLLs are found in many parts of the world including Australia, New Zealand, South Africa, South America and South-western parts of India and Sri Lanka (Hadwen, 2006). In Australia, ICOLLs are mostly located along the southeast coast extending from southern Queensland to the east coast of Victoria, of which approximately 70% are completely enclosed embayments (Ranasinghe and Pattiaratchi, 2003).

ICOLLs have distinctive physical, chemical and biological characteristics. Their shallow nature (typically <5 m) results in a high sediment surface area to water volume ratio, which increases the relative importance of sediment-water column interactions (Tyler et al. 2001). In some cases where the ICOLL basin is elevated, opening of the entrance berm may completely drain the ICOLL (Schallenberga et al., 2010). Salinity in these systems can vary significantly, from fresh to brackish to hypersaline, depending upon the amount of freshwater input, the climate and the frequency and duration of entrance opening (Ridden and Adams, 2008). Since ICOLLs can act as an accumulation basin and are flushed only periodically, they can be vulnerable to anthropogenic activities, and are considered among the most sensitive estuary type to anthropogenic disturbance (Haines, 2006; Boyd et al. 1992). They are often perceived as a surface expression of shallow aquifers and are thought to be fed by groundwater seepage during most of the year (Chikita et al., 2015) and as such they may be vulnerable to minor changes in catchment and groundwater hydrology. However, our knowledge about the relative contribution of groundwater seepage to ICOLL water budgets remains very limited.

Most previous studies on ICOLLs have focused on the influence of surface water inputs (Chikita et al., 2015, Morris and Turner, 2011). Surface water contributions to the total water budget of ICOLLs can be minimal although can be influenced by a range of factors including sediment permeability. The lack of previous groundwater studies in ICOLLs may be as a result of the inherent difficulty in quantifying groundwater seepage due to the patchy, diffuse,

and temporally variable nature of groundwater discharge (Santos et al. 2008). Attempts to resolve a nutrient mass balance in an ICOLL in South Africa were hindered by lack of data on groundwater discharging into the ICOLL (Human et al., 2015). Similarly, the nutrient loads into two ICOLLs in New Zealand were likely underestimated because the groundwater discharge was not included (Schallenberg et al., 2010). In order to advance our understanding of ICOLL hydrology and biogeochemistry, it is therefore necessary to quantify the role of groundwater discharge to ICOLL water budgets.

Natural geochemical tracers such as radon (^{222}Rn) are increasingly being used to quantify groundwater discharge and investigate its effect on water budgets and water quality (Schubert et al., 2011). The main advantage of using natural geochemical tracers is that they integrate different groundwater pathways, which is useful in spatially heterogeneous and temporally dynamic systems (Stieglitz et al., 2010, Burnett et al., 2006). Radon normally occurs in higher concentrations in groundwater relative to surface water, and the decay rate of the radon (half-life = 3.8 days) is on the same temporal scale as many of the physical processes related to groundwater discharge (Burnett et al., 2008). By assessing ^{222}Rn concentrations in groundwater and the water column, it is possible to estimate the amount of groundwater discharge to coastal surface waters. This is often achieved by mass balance approaches, originally introduced by Cable et al. (1996) and refined by multiple authors over the years (Burnett and Dulaiova, 2003; Santos et al., 2010; Burnett et al., 2010; Tait et al., 2013; Sadat-Noori et al., 2015). However, using a ^{222}Rn mass balance approach to estimate groundwater fluxes has yet to be attempted in an ICOLL system.

This study uses a radon mass balance to quantify groundwater discharge into two ICOLLs (and a nearby wetland) on Bribie Island, Australia. We hypothesize that groundwater plays a major role in the hydrology of the ICOLLs. To determine the importance of groundwater in these systems, we mapped the groundwater discharge points of entry into the ICOLLs using ^{222}Rn, and quantified the groundwater discharge into the ICOLLs over four seasons.

2. Methods

2.1. Site Description

Bribie Island (27.00˚S; 153.12˚E) is a large sand barrier island, located off the south east coast of Queensland, Australia (Figure 1). Bribie Island contains four ICOLLs, of which

Welsby and Mermaid were investigated in this project (Figure 1). South Welsby is located between these two ICOLLs and has similar characteristics to the two studied ICOLLs. However, South Welsby is classified as a coastal wetland as it does not open to the ocean, and was selected as a control site. The wetland (26.977˚S; 153.156˚E) is 150 m long, 15 m wide, has an average depth of 0.3 m and is about 150 m inland from the coastal sand dunes. Welsby ICOLL (26.965˚S; 153.154˚E) is about 0.7 km long, a maximum 40 meters wide and has an average depth of 0.4 m. Mermaid ICOLL (27.003˚S; 153.167˚E) is 1.3 km long, 70 m wide and has an average depth of about 0.4 m (Figure 1).

Bribie Island has a maximum elevation of less than 10 m with much of the island being either just above or below the water table, which has led to the creation of an extensive system of wetlands. The island is a sub-catchment of the Pumicestone regional catchment, covers an area of approximately 150 km^2, is around 30 km long and ranges from 5 to 7.5 km wide. Bribie Island has a subtropical climate with cooler, dry winters and warmer, wetter summers. Average annual rainfall on Bribie Island is 1420 mm with the majority (~60%) occurring over summer and spring periods. Over the course of this study, summer (Dec-Feb), autumn (Mar-May), winter (Jun-Aug) and spring (Sep-Nov) had seasonal rainfall of 191, 293, 201 and 160 mm, respectively (www.bom.gov.au). Urban development covers the southern end of the island with the remainder of the island consisting mainly of national park, proposed national park and state forest plantation. Pine plantation is currently being re-established in the centre of the island. National park covers 5580 ha, or approximately 40% of the island. Major vegetation types on the island are melaleuca open forest and wetland, and heath. The western side of the island supports extensive areas of intertidal mudflats, saltmarshes, mangroves and seagrasses (James and Bulley, 2004). The eastern edge of the island supports fire-sensitive beach ridge scrub and dune communities, and is also a Ramsar Wetland (Wetland of International Importance).

The groundwater resources of the island are divided into two water bodies. There is a regional surficial sand aquifer (shallow) which overlays a basal semi-confined aquifer (deep). The two aquifer units are separated by an indurated sand layer of varying thickness, porosity, and conformity throughout the Island. Water levels in the shallow aquifer follow the topography and groundwater occurs under unconfined conditions. For a full description of the Bribie Island aquifer system see Spring (2006). Groundwater in Bribie Island responds rapidly to rainfall as a result of the highly permeable sands (Armstrong, 2006). The high permeability of the sands and the low, flat topography restrict surface water runoff, with surface water only occurring as highly ephemeral streams, marshy swales and coastal

lagoons. The only significant surface water flow occurs after heavy rainfall periods (Spring, 2006). This study focussed on the eastern shoreline of Bribie Island. On the eastern coast, there is a narrow strip of foredunes. These dunes are approximately 10 m high and protect the coastal lagoons situated immediately behind them (Armstrong, 2006).

2.2. Surface water surveys

Four sampling campaigns were performed in 2014 to enable seasonal comparison of groundwater discharge (5-7 February; 2-4 May; 12-14 August and 27-29 October). Automated radon monitors (RAD7, Durridge Co.) were used which averaged ^{222}Rn concentrations over 10 min intervals giving 2-σ uncertainties of 20–30% for each data point. The instrumentation was deployed on a small kayak and moved around the ICOLLs with a GPS marking the location of the readings. To measure ^{222}Rn, a constant stream of surface water was pumped at approximately 3 L min^{-1} into a gas equilibration exchanger (Dulaiova et al., 2005). The equilibrated air was then pumped in a closed-loop from the headspace of the equilibrator chamber, through Drierite desiccant, and into the radon monitor. The partitioning of radon between the gas and the liquid phase was calculated as a function of temperature and salinity (Schubert et al., 2012). The radon activities are determined by counting the alpha-emitting, positively charged radioactive daughters (^{218}Po and/or ^{214}Po), which are detected via a silicon detector (Schubert et al., 2006). Here, we measured ^{218}Po only, as it has a secular equilibrium time of about 15 min. The ^{222}Rn measurements were corrected assuming a time lag of 20 minutes (Stieglitz et al. 2010). This assumption is based on the time-lag of radon-in-air detectors relative to radon-in-water concentration, as the time required to detect a change in ^{222}Rn activity in water varies from that in air, based on the pumping rate of water and the equilibration time in the RAD7 monitor of differing concentrations of ^{222}Rn (Petermann and Schubert, 2015).

2.3. ^{222}Rn diffusive and ^{226}Ra decay experiments

For determining ^{222}Rn diffusion from sediments, three sediment core samples were taken from each ICOLL and incubated in 60 cm long and 10 cm diameter cylinders. The cores were sealed and incubated with radium free water and left for a period of 1 month. This experiment was based on the assumption that after a month (i.e. > 5.5 half-lives for ^{222}Rn), the only source of ^{222}Rn (diffusion) will reach secular equilibrium with the only sink of ^{222}Rn (decay) within the core (Santos and Eyre, 2011). Since diffusion driven radon concentrations will

decrease with distance from the sediments (Várhegyi et al. 2013), the entire volume of water in the incubation cylinder was extracted into a six-liter gas tight bottle to prevent any concentration gradient effects. Thereafter, ^{222}Rn concentration in the water column was measured using a RAD7 closed loop system from the bottom up preventing any effects of heterogeneity within the core. (Lee and Kim, 2006).

Additionally, diffusion was independently calculated using a depth-independent approach following Equation (1) (Martens et al., 1980).

$$J_{dif} = (\lambda D_s)^{1/2} (C_{eq} - C_w) \quad (1)$$

where λ is the ^{222}Rn decay constant (0.181 day^{-1}); D_s is the effective wet bulk sediment diffusion coefficient in sediment (m^2 d^{-1}). C_{eq} is the average ^{222}Rn concentration in groundwater (Bq m^{-3}) and C_w is the average ^{222}Rn concentration in the overlying surface water (Bq m^{-3}) (Corbett et al., 1998). We calculated D_s as a function of temperature $D_s = \phi \cdot (10^{-[(980/T) + 1.59]})$ (Ullman and Aller, 1982), while porosity (ϕ) was considered 0.4 based on sediment grain density (Armstrong, 2006).

To estimate the source of radon to the water column due to the decay of dissolved radium (^{226}Ra), approximately 40 L of water was collected from each ICOLL and passed through manganese impregnated fibre at 1 L min^{-1}, which quantitatively absorbs the radium from the water (Moore and Arnold, 1996; Burnett et al., 2006). The filters were then rinsed with radium free water, partially dried and left for at least one month before being placed in the a Radium Delayed Coincidence Counter (RaDeCC) for ^{226}Ra concentration analysis (Peterson et al., 2009).

2.4. Groundwater sampling

Groundwater samples were collected seasonally from eight monitoring wells (all located in the upper aquifer) to characterize the composition of the groundwater seeping into the ICOLLs. The wells were installed by the Queensland Bulk Water Supply Authority (Seqwater) and located throughout the catchment (Figure 1). The wells ranged in depth from 4 to 19 m. In total 32 groundwater samples were collected. An inline pump was used to extract water from the wells and samples were taken after the wells were purged the equivalent of at least three times the well volume. A calibrated handheld multi-parameter probe (YSI) was used to determine salinity, pH, temperature, DO and conductivity for each sample. Gas tight six-liter plastic bottles were used to collect samples for radon analysis.

These bottles are designed to prevent gas loss and ^{222}Rn assessment can be immediately started in the field after sampling (Stringer and Burnett, 2004). Each six-liter bottle was connected to a RAD7 radon monitor and given at least two hours to achieve an air-water radon equilibrium with <5% uncertainty following well established protocols (Lee and Kim, 2006). The RAD7 was purged with dry fresh air for at least 30 min before running each sample to deplete all residual ^{222}Rn. Additionally, the sample water in each bottle was well mixed during measurements through RAD7 (Lee and Kim, 2006).

2.5. Radon mass balance

To estimate groundwater discharge into the lagoons, a ^{222}Rn mass balance model described by Dimova et al. (2013) and Perkins et al. (2015) was applied. The model accounts for all known sources and sinks of ^{222}Rn entering and leaving the system and assumes the missing ^{222}Rn is due to groundwater discharge. The sources include ^{222}Rn delivered by groundwater discharge, ^{222}Rn diffusion from sediments and ^{222}Rn ingrowth from its parent isotope ^{226}Ra while the sinks consist of radioactive decay and atmospheric loss of ^{222}Rn. A conceptual model illustrating these sources and sinks is shown in Figure 2. The mass balance model applied for estimating groundwater discharge into lakes or lagoons assuming steady-state conditions is as below (Perkins et al., 2015):

$$(F_{gw} \cdot Rn_{gw}) + (D_{dif} \cdot A) + (^{226}Ra \cdot \lambda_{222} \cdot V) = (^{222}Rn \cdot \lambda_{222} \cdot V) + J_{atm} \quad (2)$$

where F_{gw} is the groundwater discharge ($m^3\ d^{-1}$); Rn_{gw} is the groundwater endmember ^{222}Rn concentration (Bq m^{-3}); D_{dif} is ^{222}Rn diffusive flux (Bq $m^{-2}\ d^{-1}$); A is the ICOLL surface area (m^2); $^{226}Ra\ \lambda_{222}V$ is radium decay (Bq d^{-1}) where ^{226}Ra is radium concentration in the water column, λ_{222} is radon decay constant and V is the volume of water in ICOLL; $^{222}Rn\lambda_{222}V$ is the radon decay (Bq d^{-1}) where ^{222}Rn is the ^{222}Rn concentration in the water column and J_{atm} is ^{222}Rn atmospheric evasion (Bq d^{-1}). To calculate the groundwater flux for each ICOLL in each season the area weighted average surface radon concentration was used. This was used to prevent any bias resulting from small areas with high radon activity. This was done in ESRI ARCGIS 9.3 by using the average pixel value of the interpolated radon concentration map for each ICOLL in each season.

Radon flux to the atmosphere depends on molecular diffusion generated by concentration gradients and turbulent transfer, which is dependent on physical processes (Macintyre et al., 1995). The evaluation of ^{222}Rn loss to the atmosphere is based on an empirical equation that

relates the gas–water exchange to solubility (as a function of temperature and salinity), wind velocity, and the air–water ^{222}Rn gradient (Macintyre et al., 1995). The ^{222}Rn atmospheric evasion flux (J_{atm}) was estimated as follows:

$$J_{atm} = k\,(C_w - \alpha C_{air})\,A \quad (3)$$

where C_w and C_{air} are the ^{222}Rn concentrations in water and air, respectively; A is ICOLL area (m^2); α is the Ostwald solubility coefficient (dimensionless) describing the distribution of ^{222}Rn at equilibrium as the fluid to-gas ratio; and k is the piston velocity or the measure of the velocity of gas transfer at the air–water boundary (m d^{-1}). Piston velocity (k) driven by winds were estimated separately for each lagoon using (Wanninkhof 1992):

$$k_{600\,wind} = 0.45u^{1.6}(Sc/600)^{-a} \quad (4)$$

where u is wind speed (m s^{-1}); Sc is the Schmidt number for ^{222}Rn at a given water temperature; and a is a variable power function dependent on wind speeds (a = 0.6667 for u < 3.6 m s^{-1}, and a = 0.5 when u > 3.6 m s^{-1}). The Schmidt number (Sc) was calculated based on formulations given by MacIntyre et al. (1995). Wind speed data were acquired from the Australian Bureau of Meteorology (www.bom.au) from the closest weather station (Beerburrum Forest Station) located 15 km away. The uncertainty of the ^{222}Rn mass balance was calculated as a function of each individual term following the basic rules for error propagation. ICOLL areas were measured using satellite imagery imported from google earth and digitized in GIS. Depths were determined by taking the average of 10 random locations within each ICOLL.

3. Results

3.1. Environmental conditions

The region's annual total rainfall for 2014 was 875.4 mm (www.bom.gov.au), which is about 40% lower than the average annual rainfall for Bribie Island (1420 mm y^{-1}). The dry conditions throughout the year prevented any opening of the ICOLLs and therefore there was no visible water exchange between the ICOLLs and the ocean over the entire course of the

study. Antecedent rainfall totals over the previous 10 years show dry conditions prevail in the winter and spring seasons (Table 1).

3.2. Welsby ICOLL

Radon distribution varied spatially and temporally in Welsby ICOLL (Figure 3) with the highest concentrations observed in winter (up to ~ 54.5 Bq m^{-3}) followed by autumn (up to 53.7 Bq m^{-3}) (Table 2). During the summer, maximum ^{222}Rn concentrations were 2.5 times lower than winter. The higher ^{222}Rn concentrations (up to 54.5 Bq m^{-3} in winter) in the northern area of the ICOLL in all seasonal surveys indicated a possible hotspot for groundwater discharge. This may be due to higher topography to the north of the lagoon creating a steeper hydraulic gradient. The ^{222}Rn concentrations were lower during summer indicating that higher rainfall directly over the ICOLL may cause dilution of the ICOLL water. There were hypersaline conditions (43.9 ppt) observed in summer, while Autumn had the lowest average salinity (23.4 ppt) (Table 2). The ICOLL remained closed during the monitoring period, which prevented any direct connection with the ocean. This led to hypersaline conditions despite higher rainfall in summer. This was likely due to higher summer temperatures, longer hours of sunlight and evaporation of the saline ICOLL waters following a previous inundation by seawater. There was spatial variation in salinity in the ICOLL, however there was similar distribution patterns in different seasons except for summer where higher peaks in salinity were seen (Figure 3). Both salinity and ^{222}Rn concentrations were highest in the northern parts of the ICOLL during all seasons.

3.3. South Welsby Lagoon

South Welsby Lagoon was dry in the summer and could not be surveyed. Of the other seasons, the highest ^{222}Rn concentrations were observed in winter (up to ~ 52.5 Bq m^{-3}), followed by spring and autumn (Table 2). Average ^{222}Rn concentrations in the lagoon did not vary considerably between seasons and ranged from 28.8±12.1 Bq m^{-3} in autumn to 32.5±11.8 Bq m^{-3} in winter (Table 2). The low salinities observed in the lagoon (ranging from 0.2 to 0.5 ppt) (Table 2) indicate the wetland has no connectivity with the ocean and cannot be classified as an ICOLL. The central parts (main body) of the wetland had elevated ^{222}Rn concentrations indicative of a groundwater discharge hotspot (Figure 4).

3.4. Mermaid ICOLL

Similar to Welsby Lagoon, Mermaid ICOLLwas closed during the entire duration of this study. This ICOLL had the lowest average surface water ^{222}Rn concentrations (average yearly ^{222}Rn concentration was 22.8±7.4, 30.6±10.5 and 13.7±4.0 Bq m^{-3} ±SE for Welsby, South Welsby and Mermaid, respectively). In contrast to the other two systems where ^{222}Rn was highest in winter, Mermaid ICOLL had the highest ^{222}Rn concentrations in spring (up to ~ 35.2 Bq m^{-3}) followed by autumn. This suggests the three systems do not necessarily follow the same seasonal groundwater discharge pattern, despite their close proximity. Salinity in Mermaid ICOLL had large temporal changes ranging from fresh in August (winter) to hypersaline in summer (Table 2), and had the highest average salinity among all the studied systems (34.5±2.4 ppt). The spatial distribution of ^{222}Rn indicated that different areas of this ICOLL could potentially be groundwater discharge hotspots. The northern part of the ICOLL had relatively high ^{222}Rn concentrations in every survey with higher topography in that area likely driving groundwater discharge. Additionally, high ^{222}Rn concentrations in the small channels located in the middle parts of the ICOLL indicate groundwater seepage areas with groundwater likely entering the ICOLL from the west side and diluting as it moves towards the eastern side (Figure 5).

3.5. ^{222}Rn diffusion

The estimated values using the depth independent approach were on average 0.7 Bq m^{-2} day^{-1}, which is 60% lower than the average value estimated from sediment cores. As such we use the diffusion estimates from the core incubations throughout the mass balance, to provide a more conservative estimate of groundwater flow. Moreover, the peclet number defined as the advection to diffusion ratio was calculated to be 11.2 (average for two ICOLLs), indicting groundwater advection plays the major role in delivering groundwater to the ICOLLs, rather than diffusion.

3.6. Groundwater observations

Radon concentrations in groundwater samples ranged from 326 to 4019 Bq m^{-3}. The average groundwater ^{222}Rn concentrations in all the seasons was 944 ± 171 (± SE) Bq m^{-3} (n= 32) (Table 3). Average ^{222}Rn concentrations varied in each season and were 1371±375, 377±75, 395±80 and 595±119 Bq m^{-3} ± SE (n=8) in summer, autumn, winter and spring respectively. Average ^{222}Rn concentrations in groundwater were 1–2 orders of magnitude higher than in the ICOLL surface waters (Table 4). Average ^{222}Rn groundwater concentrations from samples collected in each season were used to obtain seasonal fluxes. All

groundwater samples were fresh (salinities <0.5 ppt) and no correlations were observed between ^{222}Rn and salinity in groundwater (not shown).

4. Discussion

4.1. Quantifying groundwater discharge rates

The radon mass balance quantified the known ^{222}Rn sources (i.e., diffusion from sediments and ^{226}Ra decay) and sinks (i.e., decay and atmospheric evasion) (Table 4) with the missing term assigned to groundwater discharge. Considering the shallow depth (<0.5 m) of the ICOLLs, we assumed the water was vertically homogeneous. While higher temporal resolution data is needed to test the assumption of steady state conditions in ICOLLs, we assume the mass balance to be valid on a daily basis because the surface water level of the ICOLLs was seen to be stable during the period of sampling. Using wind speeds averaged over the previous 24 h, the radon mass balance revealed average groundwater discharge rates of 3.4±2.1, 7.3±8.9 and 2.6±1.7 cm d^{-1} for Welsby, South Welsby and Mermaid, respectively (Table 5). The highest rate of groundwater discharge occurred during autumn into South Welsby Lagoon (12.5±10.6 cm d^{-1}) followed by Welsby ICOLL (5.1±3.0 cm d^{-1}) in winter. Overall, the model was highly sensitive to atmospheric losses, with evasion rates and associated uncertainties at least one order of magnitude higher than any other mass balance term (Table 4). Previous investigations of groundwater discharge into lakes have also found wind evasion to be the most important component in the radon mass balance (Cockenpot et al., 2015; Perkins et al., 2015; Dimova et al., 2013; Corbett et al., 2000).

Previous studies using a radon mass balance to calculate groundwater discharge in lakes have used either average daily wind speed data or wind speed data at sampling time to estimate radon wind evasion. Wind speed data obtained during the time of surface water surveys was used by Dimova et al. (2013), while Kluge et al., (2012) used a long term (20 years) mean daily wind velocity to calculate evasion rates. Moreover, Gilfedder et al., (2015) suggested that by averaging wind speed measurements 5 to 10 days before sampling, more reasonable fluxes could be obtained. Here, we used the average daily wind speeds as sampling took place during the time of day when wind speeds were at their greatest. If we used wind speeds during sampling time with no localized wind attenuation at the surface of the ICOLLs, the model estimated groundwater discharge rates would increase by 147%, 63% and 165% for Welsby, South Welsby and Mermaid, respectively. In this scenario, average

estimated groundwater discharge rates would be 8.4±3.0, 11.9±5.3 and 6.9±3.5 cm d^{-1} for Welsby, South Welsby and Mermaid, respectively (Table 5). These values seem unrealistic considering the shallow nature of all ICOLLs. Wind attenuation due to vegetation surrounding wetlands may be very important (Gilfedder et al., 2015). Considering the ICOLLs are surrounded by vegetation, some wind attenuation was likely. If we assume a 50% wind attenuation, average groundwater discharge would be 1.6±1.8, 3.7±2.8 and 1.3±0.8 cm d^{-1} for Welsby, South Welsby and Mermaid, respectively. We interpret these values as minimum groundwater discharge rates for the systems investigated. If an average daily wind speed data complied of 10 days before sampling was used to estimate wind evasion effect on radon concentration, evasion rates would not vary significantly except for autumn in South Welsby and Mermaid lagoons (Table 4) when compared to the average daily wind speed 24 h prior to sampling. Therefore, both approaches will result in very similar estimates (within 10%) of groundwater discharge rates. Regardless of any assumptions on wind speeds and associated ^{222}Rn evasion, all these groundwater discharge rates are much higher than the potential surface water inputs into the ICOLLs (discussed later).

Dissolved ^{226}Ra was measured once during the study period and applied to all seasons. The ICOLLs had highly variable salinities which could contribute to varying dissolved ^{226}Ra activities (and therefore in-situ production rates for ^{222}Rn) throughout the study period. If ^{226}Ra concentrations were an order of magnitude higher during the non-sampled seasons, average annual groundwater discharge estimates would decrease by 3 to 27%. However, ^{222}Rn produced through the decay of ^{226}Ra was assumed to be negligible as the ^{226}Ra decay term has been reported previously to be a minor contributor (<5%) to the radon mass balance in coastal environments (Burnett and Dulaiova, 2003; Tait et al., 2013; Stewart et al., 2015).

Rainfall was highest during summer which corresponded with the lowest estimates of groundwater discharge. Lower rainfall during the winter coincided with higher groundwater inflow than the other seasons. Autumn had the highest groundwater discharge in South Welbsley and Mermaid ICOLLs (groundwater discharge in Welsby was fairly consistent). Summer had higher rainfall than autumn, but autumn had higher daily rainfalls than other seasons. This indicates that cumulative effect of smaller rainfall events during the month prior to survey may not efficiently recharge the groundwater system of the area as most of the rainfall happened in summer. Approximately 80% of rainfall on Bribie Island is reported to be lost through evapotranspiration before any recharge (Armstrong, 2006).

4.2. Groundwater role in ICOLLs hydrology

411 The estimated groundwater discharge rates indicate that groundwater contributed
412 between 1% and 31% of the ICOLLs water volume in a day (i.e. groundwater discharge
413 divided by ICOLL volume). There is limited surface water runoff into the ICOLLs on Bribie
414 Island (Spring, 2006), and no surface flows were observed during the field investigations. A
415 comparison between the average local annual precipitation (1420 mm y^{-1}) and the average
416 annual groundwater discharge rates for each lagoon (12410, 26645, 9490 mm y^{-1}) revealed
417 that groundwater input to the ICOLLs was equal to 89%, 94% and 87% of the total (rainfall +
418 groundwater) annual water input, for Weslby, South Weslby and Mermaid, respectively.
419 These estimates demonstrate that groundwater discharge plays a major role in the hydrology
420 of Bribie Island ICOLLs. A decrease in groundwater levels may result in longer recharge
421 times, leading to lower surface water levels that may potentially change the opening and
422 closing regime of the ICOLLs. Although we did not observe surface runoff into the ICOLLs
423 during sampling campaigns, it is likely that surface water inputs occur during heavy rain
424 events when the sand becomes saturated (Armstrong, 2006). Additionally, some seepage is
425 expected to occur from the ICOLL to the ocean due to the permeable berm and hydraulic
426 gradient.
427 Since the ICOLLs were closed during our field investigations, we compare our
428 observations to groundwater discharge estimates from a range of terrestrial and coastal lakes
429 to put the results in perspective (Table 6). However, consideration must be given to the
430 potential morphological differences between the study of ICOLLs and other lake systems due
431 to the high permeability of the sandy sediment underlying the ICOLLs. Past studies in lakes
432 have shown that a low proportion (<1%) of lake water was replaced daily by groundwater
433 discharge (Table 6). A recent review showed that median groundwater discharge rate into 107
434 lakes was 0.74 cm d^{-1} (Rosenberry et al., 2015). Our estimated average annual groundwater
435 inflow is eight-fold higher than this average global rate. The higher proportion of
436 groundwater discharge in ICOLLs may in part be due to the ratio of shoreline to lake volume.
437 This ratio in previous studies of lakes was <0.006, however in this study the ratio was 0.046,
438 1.019 and 0.23 for Welsby, South Welsby and Mermaid Lagoon, respectively (Table 6;
439 Figure 6). Higher shoreline to volume ratio may increase the relative contribution of
440 groundwater discharge (Santos et al., 2012b). However, in most of these past studies,
441 groundwater discharge exceeded direct rainfall input, demonstrating the importance of
442 groundwater discharge in the hydrology of lakes.
443 There was a general negative relationship between surface lake area and the groundwater
444 discharge to rainfall ratio over an annual cycle suggesting that even if groundwater discharge

445 rates are small (because seepage is occurring over a large lake surface water area) they are a
446 very important component to the lake water budgets. This highlights that groundwater is
447 relatively more important than rainfall in the hydrology of ICOLLs (due to smaller surface
448 area and shallow depth) and can have higher relative fluxes than other types of lakes. The
449 high discharge in ICOLLs could also be due to the high hydraulic conductivity of the aquifer
450 in this area. Previous studies have reported hydraulic conductivity values for Bribie Island
451 ranging from 7 to 25 m d^{-1} (Harbison and Cox, 1998; Armstrong, 2006; Spring, 2006). The
452 well-sorted sands with high permeability and dunes overlying the regional aquifer are likely
453 the main reason for this high conductivity. In other sandy coastal lagoons, a similar
454 groundwater flux (6 cm d^{-1}) to that observed in this study (between 2.6 and 7.3 cm d^{-1}) has
455 been reported (El-Gamal et al., 2012) (Table 6).
456 Calculated groundwater discharge rates are directly related to the radon concentration of
457 the groundwater end-member meaning that higher radon concentrations in groundwater
458 would result in lower groundwater discharge rates. Our radon end-member concentration was
459 within the range of previous studies in regional shallow coastal aquifers along Australia's
460 east coast (Perkins et al., 2014; Makings et al., 2014; Gleeson et al., 2013, Maher et al., 2013,
461 Atkins et al., 2013), but is lower than those reported in other coastal environments elsewhere
462 (Dimova et al., 2013; Peterson et al., 2010).
463 Moreover, groundwater discharge for each ICOLL was calculated using the total area of
464 each ICOLL. As the soil surrounding the ICOLLs is very permeable there is likely
465 groundwater exchange across the barrier between the ICOLLs and the ocean which would be
466 driven by differential pressure heads. This subsurface outflow means that the actual
467 groundwater flux would be larger than the values reported since this subsurface groundwater
468 loss term was not considered in the mass balance calculations. In future research, the
469 installation of piezometers may help determine gaining and losing zones in the ICOLLs and
470 provide information on the magnitude of head gradients and water losses through the
471 permeable berm separating the ICOLLs from the ocean.
472
473 **4.3. A tentative conceptual model**
474 Our observations offer some conceptual insight into ICOLL hydrology as summarized in
475 Figure 7. Radon may enter ICOLLs via fresh groundwater discharge driven by local
476 hydraulic gradients and shallow porewater exchange driven by convection. ICOLLs often
477 open during periods of high rainfall. Following the rainfall, seawater infiltrates the ICOLL at
478 high tide. As this saline water in the ICOLLs is subject to evaporation in warmer, drier

periods, with low fresh groundwater discharge, it becomes hypersaline. The difference in density between the overlying hypersaline waters and the brackish porewater can drive convective exchange at the sediment water interface and create salt fingers (Webster et al., 1996). This coupled with lower groundwater levels in drier periods would allow saline surface waters to permeate bottom sediments. While we have no salinity data in shallow ICOLL porewaters to test this hypothesis, previous studies have shown convection-driven bottom water recirculation into estuaries sediments (Santos et al., 2012a; Robinson et al., 2007; Webster et al., 1996) and have mentioned the potential importance of this process (Rocha, 2000; Santos et al., 2012b; Maher et al., 2015).

With the discharge of ^{222}Rn enriched fresh groundwater into saline surface waters, a negative relationship between groundwater discharge and salinities was found (Figure 8) as has also been reported for other coastal lagoons (Su et al., 2014; El-Gamal et al., 2012). In both Welsby and Mermaid ICOLLs, groundwater discharge was lower in summer (high evaporation) while salinity was at its highest. These ICOLLs were closed to the ocean over the study period but have the highest salinity in the first sampling period (summer) indicating saltwater (ocean water) intrusion shortly before the commencement of the study. During wetter times, when groundwater levels rise, the shallow brackish to hypersaline porewater (now enriched in ^{222}Rn) under the ICOLL may be forced back into surface waters creating localised ^{222}Rn hotspots with high salinity. To explain these instances of the localised coupling of high salinity and high radon concentrations, we present a conceptual model. As ICOLLs are shallow in nature (< 40 cm) and bottom sediments are made up of coarse sands, recirculation of the surface waters may be significant. This can occur through drivers such as density driven porewater exchange, bioirrigation and bioturbation (Santos et al., 2012) which cause surface water to infiltrate into the sediment, picking up a radon signal and discharging back into surface waters. However, the inverse relationship between salinity and groundwater discharge rates (Figure 8) implies a second scenario that fresh groundwater discharge (rather than saline porewater exchange) dominated ^{222}Rn sources during our investigations. Radon acts as a tracer for both fresh groundwater flux and recirculated groundwater flux.

We are unable to quantitatively separate the relative contribution of fresh groundwater discharge versus saline porewater exchange driven by convection using ^{222}Rn data only. Since fresh groundwater would be a source of new nutrients, and porewater would be a source of recycled nutrients (Weinstein et al., 2011), we suggest future studies use a combination of chemical tracers such as radium to resolve the contribution of these two water pathways to biogeochemical cycles in ICOLLs.

5. Conclusions

This study relied on the natural geochemical groundwater tracer ^{222}Rn to quantify groundwater inflow into a coastal wetland and two ICOLLs. There was substantial spatial and temporal variability in ^{222}Rn concentrations within the lagoons. The radon mass balance approach provided evidence that groundwater supplies a significant proportion of the recharge to Welsby, South Welsby and Mermaid Lagoons on Bribie Island with an average annual groundwater discharge rates of 3.4±2.1, 7.3±8.9 and 2.6±1.7 cm d^{-1} respectively. The estimated groundwater discharge rate in the ICOLLs was much larger than has been reported in other lake systems probably because of the high permeability of surrounding soils and the high shoreline to lake volume ratio in ICOLLs. Over the study period, ~ 90% of water inputs to the ICOLLs were of comprised of groundwater, demonstrating that the hydrology of Bribie Island ICOLLs is dominated by groundwater discharge.

Acknowledgements

We would like to thank Paul Macklin for his contribution during field campaigns and data collection. Funding for this research project was provided by Queensland Bulk Water Supply Authority (Seqwater) and the Australian Research Council (DP120101645, DE140101733, DE150100581 and LE120100156). This study was partially inspired by the CSIRO Coastal Carbon Cluster. Advice by Andrew Smolders, Cameron Veal and Morag Stewart prior and during field investigations is appreciated.

References

ARMSTRONG, T.J. 2006. Determination of aquifer properties and heterogeneity in a large coastal sand mass: Bribie Island southeast Queensland. Queensland University of Technology, Brisbane, Queensland, Australia. pp 240.

ATKINS, M. L., I. R. SANTOS, S. RUIZ-HALPERN AND D. T. MAHER 2013. Carbon dioxide dynamics driven by groundwater discharge in a coastal floodplain creek. Journal of Hydrology 493: 30-42.

BOYD, R. DALRYMPLE, R., ZAITLIN, B.A. 1992. Classification of clastic coastal depositional environments. Journal of Sedimentary Petrology. 62, 569-583.

BURNETT, W. C. & DULAIOVA, H. 2006. Radon as a tracer of submarine groundwater discharge into a boat basin in Donnalucata, Sicily. Continental Shelf Research, 26, 862-873.

BURNETT, W. C., BOKUNIEWICZ, H., HUETTEL, M., MOORE, W. S. 2003. Groundwater and pore water inputs to the coastal zone. Biogeochemistry. 66, 3–33.

550 BURNETT, W. C., PETERSON, R. N., SANTOS, I. R. & HICKS, R. W. 2010. Use of
551 automated radon measurements for rapid assessment of groundwater flow into
552 Florida streams. Journal of Hydrology, 380, 298–304.
553 BURNETT, W. C., PETERSON, R., MOORE, W. S. & DE OLIVEIRA, J. 2008. Radon and
554 radium isotopes as tracers of submarine groundwater discharge–results from the
555 Ubatuba, Brazil SGD assessment intercomparison. Estuarine, Coastal and Shelf
556 Science, 76, 501-511.
557 CABLE, J. E., BURNETT, W. C., CHANTON, J. P. & WEATHERLY, G. L. 1996.
558 Estimating groundwater discharge into the northeastern Gulf of Mexico using
559 radon-222. Earth and Planetary Science Letters, 144, 591-604.
560 CHIKITA, K. A., UYEHARA, H., AL-MAMUN, A., UMGIESSER, G., IWASAKA, W.,
561 HOSSAIN, M. M., SAKATA, Y., 2015. Water and heat budgets in a coastal
562 lagoon controlled by groundwater outflow to the ocean. Limnology, DOI
563 10.1007/S10201-015-0449-4.
564 COCKENPOT, S., CLAUDE, C., RADAKOVITCH, O. 2015. Estimation of air-water gas
565 exchange coefficient in a shallow lagoon based on ^{222}Rn mass balance. Journal of
566 Environmental Radioactivity, 14, 58–69.
567 CORBETT, D.R., DILLON, K., BURNETT, W., CHANTON, J. 2000. Estimating the
568 groundwater contribution into Florida Bay via natural tracers, 222Rn and CH4.
569 Limnology & Oceanography 45(7):1546–1557
570 DIMOVA, N.T. AND BURNETT, W.C., 2011. Evaluation of groundwater discharge into
571 small lakes based on the temporal distribution of radon-222. Limnology and
572 Oceanography, 56(2): 486-494.
573 DIMOVA, N.T., BURNETT, W.C., CHANTON, J.P., CORBETT, J.E. 2013. Application of
574 radon-222 to investigate groundwater discharge into small shallow lakes. Journal
575 of Hydrology 486, 112–122.
576 DULAIOVA, H., PETERSON, R., BURNETT, W. C. & LANE-SMITH, D. 2005. A multi-
577 detector continuous monitor for assessment of 222Rn in the coastal ocean. Journal
578 of Radioanalytical and Nuclear Chemistry, 263, 361–365.
579 EL-GAMAL, A. A., PETERSON, R. N., BURNETT, W. C., 2012. Detecting Freshwater
580 Inputs via Groundwater Discharge to Marina Lagoon, Mediterranean Coast, Egypt.
581 Estuaries and Coasts, 35:1486–1499.
582 GILFEDDER, B.S., FREI, S., HOFMANN, H., CARTWRIGHT, I. 2015. Groundwater
583 discharge to wetlands driven by storm and flood events: Quantification using
584 continuous Radon-222 and electrical conductivity measurements and dynamic
585 mass-balance modelling. Geochimica et Cosmochimica Acta. 165, 161‑177.
586 GLEESON, J., SANTOS, I.R., MAHER, D.T., GOLSBY-SMITH, L., 2013. Groundwater‑
587 surface water exchange in a mangrove tidal creek: evidence from natural
588 geochemical tracers and implications for nutrient budgets. Mar. Chem., 156
589 HADWEN, W. L. 2006. Ecology, threats and management options for small estuaries and
590 ICOLLS. *Sustainable Tourism Cooperative Research Centre.* Technical Report.
591 HAINES, P. E. 2006. Physical and chemical behaviour and management of Intermittently
592 Closed and Open Lakes and Lagoons (ICOLLs) in NSW. Gold Coast: Griffith
593 University, Ph.D. thesis, 505p.
594 HAINES, P. E., TOMLINSON, R. B., THOM, B. G., 2006. Morphometric Assessment of
595 intermittently open/closed coastal lagoons in New South Wales, Australia.
596 Estuarine, Coastal and Shelf. Science 67(1-2), 321-332.

HARBISON, J., COX M.E., 1998. General features of the occurrence of groundwater on Bribie Island, Moreton Bay and catchment. School of Marine Science, University of Queensland, Brisbane.

HUMAN L. R. D., Snowb G. C., Adamsa J. B., Batea G. C., Yangc, S.-C. 2015. The role of submerged macrophytes and macroalgae in nutrient cycling: A budget approach. Estuarine, Coastal and Shelf Science. 154, 169‑178.

JAMES R. AND BULLEY G. 2004. Fire management system report. Queensland Government, Queensland Parks and Wildlife Services.

KLUGE, T., ILMBERGER, J., VON ROHDEN, C., AESCHBACH-HERTIG, W. 2007. Tracing and quantifying groundwater inflow into lakes using radon-222. Hydrology and Earth System Sciences. 11(5), 1621–1631.

KLUGE, T., VON ROHDEN, C., SONNTAG, P., LORENZ, S., WIESER, M., AESCHBACH-HERTIG, W., ILMBERGER, J. 2012. Localising and quantifying groundwater inflow into lakes using high-precision ^{222}Rn profile. Journal of Hydrology, 450–451, 70–81.

LEE, J. M., KIM, G. 2006. A simple and rapid method for analyzing radon in coastal and ground waters using a radon-in-air monitor. Journal of Environmental Radioactivity, 89, 219-228.

MACINTYRE, S., WANNINKHOF, R., CHANTON, J. 1995. Trace gas exchange across the air-water interface in freshwater and coastal marine environments. Biogenic trace gases: Measuring emissions from soil and water, Blackwell Science Ltd. 52-97.

MAHER, D. T., I. R. SANTOS, L. GOLSBY-SMITH, J. GLEESON AND B. D. EYRE 2013. Groundwater-derived dissolved inorganic and organic carbon exports from a mangrove tidal creek: The missing mangrove carbon sink? Limnology and Oceanography 58(2): 475–488.

MAHER, D.T., COWLEY, K., SANTOS, I.R., MACKLIN, P.A. AND EYRE, B.D., 2015. Methane and carbon dioxide dynamics in a subtropical estuary over a diel cycle: Insights from automated in situ radioactive and stable isotope measurements. Marine Chemistry, 168: 69-79.

MAKINGS, U., SANTOS, I.R., MAHER, D.T., GOLSBY-SMITH, L., EYRE, B.D., 2014. Importance of budgets for estimating the input of groundwater-derived nutrients to an eutrophic tidal river and estuary. Estuar. Coast. Shelf Sci. 143, 65‑76.

MARTENS, C.S., KIPPHUT, G.W., KLUMP, J.V., 1980. Sediment–water chemical exchange in the coastal zone traced by in situ radon- 222 flux measurements. Science 208, 285–288.

MOORE, W. S. & ARNOLD, R. 1996. Measurement of 223Ra and 224Ra in coastal waters using a delayed coincidence counter. Journal of Geophysical Research: Oceans (1978–2012), 101, 1321-1329.

MORRIS, B., D., TURNER I., L., 2011. Morphodynamics of intermittently open–closed coastal lagoon entrances: New insights and a conceptual model. Marine Geology, Volume 271: 55–66.

PERKINS A. K., SANTOS, I. R. SADAT-NOORI, M. GATLAND, J. R. MAHER, D. T. 2015. Groundwater seepage as a driver of CO_2 evasion in a coastal lake (Lake Ainsworth, NSW, Australia). Environmental Earth Sciences. DOI 10.1007/s12665-015-4082-7

PETERMANN, E., SCHUBERT. M. 2015. Quantification of the response delay of mobile radon-in-air detectors applied for detecting short-term fluctuations of radon-in-water concentrations. The European Physical Journal - Special Topics 224, 697–707.

PETERSON, R. N., BURNETT, W. C., DIMOVA, N. & SANTOS, I. R. 2009. Comparison of measurement methods for radium-226 on manganese-fiber. Limnology and Oceanography: Methods, 7, 196–205.

PETERSON, R. N., SANTOS, I. R., BURNETT, W. C. 2010. Evaluating groundwater discharge to tidal rivers based on a Rn-222 time-series approach. Estuarine, Coastal and Shelf Science 86, 165–178.

RIDDEN, T. AND ADAMS, J.B., 2008. Influence of mouth status and water level on the macrophytes in a small temporarily open/closed estuary. Estuarine, Coastal and Shelf Science, 79, 86–92.

ROBINSON, C., L. LI, AND H. PROMMER. 2007. Tide-induced recirculation across the aquifer-ocean interface. Water Resources Research 43: W07428, doi:10.1029/2006WR005679

ROCHA, C., 2000. Density-driven convection during flooding of warm, permeable intertidal sediments: The ecological importance of the convective turnover pump. . Journal of Sea Research, 43: 1-14.

ROSENBERRY, D. O., LEWANDOWSKI, J., MEINIKMANN K. & NÜTZMANN G. 2015. Groundwater - the disregarded component in lake water and nutrient budgets. Part 1: effects of groundwater on hydrology. Hydrological Processes, 29, 2895–2921.

SADAT-NOORI, M., SANTOS, I., SANDERS, C., SANDERS, L. AND MAHER, D., 2015. Groundwater discharge into an estuary using spatially distributed radon time series and radium isotopes. Journal of Hydrology, 528, 703-719.

SANTOS I. R., EYRE, B. D., MARKUS HUETTEL, A., 2012b. The driving forces of porewater and groundwater flow in permeable coastal sediments: A review. Estuarine, Coastal and Shelf Science 98, 1-15.

SANTOS, I. R. & EYRE, B. D. 2011. Radon tracing of groundwater discharge into an Australian estuary surrounded by coastal acid sulphate soils. Journal of hydrology, 396, 246-257.

SANTOS, I. R., COOK, P. L. M., DE WEYS, L. R. J., EYRE B. D. 2012a. The ‘‘salt wedge pump’’: Convection-driven pore-water exchange as a source of dissolved organic and inorganic carbon and nitrogen to an estuary. Limnology and Oceanography, 57(5), 1415–1426.

SANTOS, I.R., ERLER, D., TAIT, D.R., EYRE, B.D., 2010. Breathing of a coral cay: Tracing tidally driven seawater recirculation in permeable coral reef sediments. Journal of Geophysical Research 115.C12.

SANTOS, I.R., NIENCHESKI, F., BURNETT, W., PETERSON, R., CHANTON, J., ANDRADE, C.F.F., MILANI, I.B., SCHMIDT, A., KNOELLER, K., 2008. Tracing anthropogenically-driven groundwater discharge into a coastal lagoon from southern Brazil. Journal of Hydrology 353, 275–293.

SANTOS, I.R., PETERSON, R.N., EYRE, B.D., BURNETT, W.C. 2010. Significant lateral inputs of fresh groundwater into a stratified tropical estuary: evidence from radon and radium isotopes. Marine Chemistry. 121, 37‑48.

SCHALLENBERG M., LARNED S.T., HAYWARD S, ARBUCKLE C. 2010. Contrasting effects of managed opening regimes on water quality in two intermittently closed and open coastal lakes. Estuarine, Coastal and Shelf Science 86, 587–597.

SCHMIDT, A., GIBSON, J.J., SANTOS, I.R., SCHUBERT, M., TATTRIE, K. 2010. The contribution of groundwater discharge to the overall water budget of two typical Boreal lakes in Alberta/Canada estimated from a radon mass balance. Hydrology Earth System Sciences, 14:79–89.

694 SCHMIDT, A., STRINGER C. E., HAFERKORN U., SCHUBERT, M. 2009. Quantification
695 of groundwater discharge into lakes using radon-222 as naturally occurring tracer.
696 Environmental Geology, 56:855–863.
697 SCHUBERT, M., BRUEGGEMANN, L., KNOELLER, K. & SCHIRMER, M. 2011. Using
698 radon as an environmental tracer for estimating groundwater flow velocities in
699 single well tests. Water Resources Research, 47, W03512,
700 doi:10.1029/2010WR009572.
701 SCHUBERT, M., PASCHKE, A., LIEBERMAN, E., BURNETT, W.C., 2012. Air‐water
702 partitioning of ^{222}Rn and its dependence on water temperature and salinity.
703 Environmental Sciences and Technology, 46, 3905‐3911.
704 SPRING, K. 2006. Groundwater flow model for a large sand mass with heterogeneous media,
705 Bribie Island South Queensland. Thesis. Queensland University of Technology,
706 Brisbane, Queensland, Australia. 187 pages.
707 STEWART, B. T., I. R. SANTOS, D. R. TAIT, P. A. MACKLIN, AND D. T. MAHER,
708 2015. Submarine groundwater discharge and associated fluxes of alkalinity and
709 dissolved carbon into Moreton Bay (Australia) estimated via radium isotopes,
710 Marine Chemistry, 174, 1-12.
711 STIEGLITZ T. C., COOK P. G. AND BURNETT W. C. 2010. Inferring coastal processes
712 from regional-scale mapping of ^{222}Radon and salinity: examples from the Great
713 Barrier Reef, Australia. Journal of Environmental Radioactivity. 101, 544–552.
714 SU, N., BURNETT, W.C., MACINTYRE, H.L., LIEFER, J.D., PETERSON, R.N., VISO,
715 R., 2014. Natural radon and radium isotopes for assessing groundwater discharge
716 into Little Lagoon, AL: implications for Harmful Algal Blooms. Estuaries and
717 Coasts 37, 893‐910.
718 TAIT, D.R., SANTOS, I.R., ERLER, D.V., BEFUS, K.M., CARDENAS, M.B., EYRE, B.D.,
719 2013. Estimating submarine groundwater discharge in a South Pacific coral reef
720 lagoon using different radioisotope and geophysical approaches. Marine Chemistry
721 156, 49-60.
722 TYLER, A. C., MCGLATHERY, K. J. AND ANDERSON, I. C. 2001. Macroalgae
723 mediation of dissolved organic nitrogen fluxes in a temperate coastal lagoon.
724 Estuarine, Coastal and Shelf Science. 53, 155-168.
725 ULLMAN, W.J., ALLER, R.C., 1982. Diffusion coefficients in nearshore marine sediments.
726 Limnology and Oceanography 27, 552–556.
727 VÁRHEGYI, A., J. SOMLAI, AND Z. SAS. 2013. Radon migration model for covering U
728 mine and ore processing tailings. Romanian Journal of Physics, 58: 298–310.
729 WANNINKHOF, R. 1992. Relationship between wind speed and gas exchange over the
730 ocean. Journal of Geophysical Research, 97, 7373–7382.
731 WEINSTEIN, Y. ET AL., 2011. What is the role of fresh groundwater and recirculated
732 seawater in conveying nutrients to the coastal ocean? Environmental Science &
733 Technology, 45(12): 5195-5200.
734
735

736 **Table 1.** Rainfall in the region the month prior to sampling over a 10 year average, one
737 month prior to sampling and one week prior to sampling.

Season	10 year average one month prior (mm)	One month prior (mm)	One week prior (mm)
Summer (5th February)	223	63	0.5
Autumn (2nd May)	160	110	31
Winter (12th August)	48	16	0
Spring (27th October)	88	13	7

738

739 **Table 2.** Maximum, minimum and average ^{222}Rn concentrations and salinity in Welsby,
740 Mermaid ICOLLs and South Welsby lagoon during each survey time.
741

		Welsby				South Welsby				Mermaid			
Summer		Min.	Max.	Ave.	Stdv.	Min.	Max.	Ave.	Stdv.	Min.	Max.	Ave.	Stdv.
	Radon (Bq m^{-3})	0.3	22.5	10.3	5.3	n.d.	n.d.	n.d.	n.d.	1.7	19.5	11.8	4.2
	Salinity	42.8	44.7	43.9	0.5	n.d.	n.d.	n.d.	n.d.	30.7	54.3	47.6	4.9
Autumn													
	Radon (Bq m^{-3})	4.5	53.7	27.2	9.7	10.3	42.3	28.8	12.1	2.5	29.4	14.2	6.8
	Salinity	17.2	18.9	18.0	0.2	0.3	0.4	0.3	0.1	22.1	24.4	23.1	3.7
Winter													
	Radon (Bq m^{-3})	2.3	54.5	29.2	11.1	9.4	52.5	32.5	11.8	0.8	25.4	9.2	6.1
	Salinity	11.7	27.4	19.5	2.1	0.2	0.4	0.3	0.1	1.8	36.2	33.6	0.5
Spring													
	Radon (Bq m^{-3})	1.3	43.2	24.5	9.5	22.4	47.1	30.6	11.9	1.1	35.2	20.0	7.9
	Salinity	18.6	24.5	21.5	2.3	0.2	0.5	0.3	0.2	32.5	35.1	33.8	0.8

742 n.d. = no data.

743 **Table 3.** Groundwater observations.

Sample No.	Date	Closest system	Lat.	Long.	Depth (m)	Temp (C)	Sal	pH	Cond. (mS cm^{-1})	DO (mg L^{-1})	^{222}Rn (Bq m^{-3})
1	6/02/2014	Welsby	S26.965	E153.144	15.6	21.7	0.1	7.6	0.1	0.3	1344
2	6/02/2014	Welsby	S26.965	E153.144	8	22	0.3	5.4	0.5	0.2	1765
3	6/02/2014	South Welsby	S26.981	E153.149	16.5	22.9	0.1	5.1	0.3	0.1	881
4	6/02/2014	South Welsby	S26.981	E153.149	6	24.6	0.1	4.8	0.3	0.1	4019
5	6/02/2014	Mermaid	S26.994	E153.156	18.8	26.4	0.1	5.6	0.2	0.2	698
6	6/02/2014	Mermaid	S26.994	E153.156	12.8	24.9	0.1	4.9	0.2	0.2	884
7	6/02/2014	Mermaid	S26.994	E153.156	10	28.3	0.1	5.6	0.3	0.4	617
8	6/02/2014	Mermaid	S26.994	E153.156	4	24.5	0.2	6.6	0.5	1.4	761
9	3/05/2014	Welsby	S26.965	E153.144	15.6	20.9	0.1	5	0.1	1	326
10	3/05/2014	Welsby	S26.965	E153.144	8	22	0.1	4.3	0.2	3.3	333
11	3/05/2014	South Welsby	S26.981	E153.149	16.5	21.4	0.1	5.2	0.2	3.2	361
12	3/05/2014	South Welsby	S26.981	E153.149	6	23.9	0.1	4.2	0.2	0.8	368
13	3/05/2014	Mermaid	S26.994	E153.156	10	21	0.2	5	0.4	0.7	389
14	3/05/2014	Mermaid	S26.994	E153.156	4	22.9	0.1	4.3	0.2	2.5	396
15	3/05/2014	Mermaid	S26.994	E153.156	18.8	21.4	0.1	4.7	0.3	1	416
16	3/05/2014	Mermaid	S26.994	E153.156	12.8	21.2	0.1	4.2	0.3	0.4	430
17	13/08/2014	Welsby	S26.965	E153.144	15.6	21.2	0.1	4.2	0.2	2.6	357
18	13/08/2014	Welsby	S26.965	E153.144	8	20.5	0.1	5.3	0.2	3.2	350
19	13/08/2014	South Welsby	S26.981	E153.149	16.5	21.3	0.1	4.5	0.2	3.2	385
20	13/08/2014	South Welsby	S26.981	E153.149	6	20.1	0.1	4.2	0.2	3.1	382
21	13/08/2014	Mermaid	S26.994	E153.156	18.8	21.8	0.1	4	0.3	2.8	416
22	13/08/2014	Mermaid	S26.994	E153.156	12.8	21.9	0.1	4.7	0.3	2.7	409
23	13/08/2014	Mermaid	S26.994	E153.156	10	21.3	0.2	4.3	0.5	2.7	434
24	13/08/2014	Mermaid	S26.994	E153.156	4	19.9	0.1	4.3	0.2	2.7	430
25	28/10/2014	Welsby	S26.965	E153.144	15.6	22.5	0.1	3.7	0.1	0.7	541
26	28/10/2014	Welsby	S26.965	E153.144	8	22.6	0.1	4.6	0.2	2.2	562
27	28/10/2014	South Welsby	S26.981	E153.149	16.5	23.7	0.1	4.3	0.2	0.3	583
28	28/10/2014	South Welsby	S26.981	E153.149	6	22	0.1	3.9	0.2	1	576
29	28/10/2014	Mermaid	S26.994	E153.156	18.8	21.8	0.1	4.4	0.3	0.3	618
30	28/10/2014	Mermaid	S26.994	E153.156	12.8	22.2	0.1	4.3	0.3	0.3	597
31	28/10/2014	Mermaid	S26.994	E153.156	10	21.2	0.2	4.6	0.5	0.3	646
32	28/10/2014	Mermaid	S26.994	E153.156	4	22.2	0.1	4.2	0.2	0.9	640
				Min.	2	19.9	0.1	3.7	0.1	0.1	326
				Max.	18.8	29.2	0.3	7.6	1.2	3.2	4019
				Ave.	10.1	22.8	0.2	4.9	0.3	1.3	944
				STDV.	5.8	2.2	0.1	0.9	0.2	1.1	968

744

745

746

747 **Table 4.** A summary of the terms used in the ^{222}Rn mass balance model in the ICOLLs.

	Welsby Lagoon				South Welsby Lagoon				Mermaid Lagoon			
	Summer	Autumn	Winter	Spring	Summer	Autumn	Winter	Spring	Summer	Autumn	Winter	Spring
Wei. Ave. SW ^{222}Rn (Bq m^{-3})	10.3±4.4	27.0±7.8	29.3±8.1	24.5±6.7	n/d	28.8±9.6	32.5±8.9	30.6±8.1	11.8±7.8	14.1±5.8	9.1±5.3	20.2±5.8
Ave. GW ^{222}Rn (Bq m^{-3})	1919.4±384.0	377.6±75.1	395.8±80.1	595.5± 119.2	1919.4± 384.0	377.6± 75.1	395.8± 80.1	595.5± 119.2	1919.4± 384.0	377.6± 75.1	395.8± 80.1	595.5± 119.2
Ave. Depth (m)	0.3±0.04	0.4±0.04	0.4±0.04	0.4±0.04	0	0.4±0.04	0.3±0.04	0.3±0.04	0.4±0.04	0.4±0.04	0.3±0.04	0.4±0.04
Ave. area (m^2)	88,386.2	88,386.2	88,386.2	88,386.2	0	4,183.1	2,000.5	2,416.3	40,521.2	67,429.2	100,132.4	34,725.1
Volume (m^3)	30,935	35,354	44,193	35,354	0	1,673	700	725	16,208	26,971	35,046	13,890
Ave. wind speed at sampling time (m s^{-1})	5.2±1.0	5.9±1.2	6.0±1.2	6.1±1.2	6.1	7.6±1.5	6.2±1.2	3.9±0.8	5.4±1.1	10.2±2.0	4.6±0.9	7.2±1.4
Ave. daily wind speed (m s^{-1})	4.2±0.8	3.3±0.7	3.6±0.7	3.9±0.8	4.1±0.8	5.8±1.2	3.9±0.8	3.1±0.6	3.0±0.6	6.1±1.2	3.9±0.8	3.1±0.6
Ave. 10 day prior to sampling daily wind speed (m s^{-1})	4.0±0.8	3.0±0.5	3.4±0.6	3.8±0.8	4.0±0.8	3.0±0.5	3.4±0.6	3.8±0.8	4.0±0.8	3.0±0.5	3.4±0.6	3.8±0.8
^{222}Rn decay (Bq m^{-2} d^{-1})	0.7±0.3	2.0±0.8	2.1±09	1.7±0.8	0	2.1±0.9	2.1±0.8	1.7±0.7	0.9±0.6	1.0±0.6	0.6±0.4	1.4±0.6
^{222}Rn evasion (Bq m^{-2} d^{-1})	2.5±0.5	17.4±3.5	21.6±4.3	27.3±7.5	0	47.4±9.5	25.4±4.1	18.7±3.7	8.1±1.6	22.5±4.5	8.3±1.7	12.1±1.4
^{226}Ra ingrowth (Bq m^{-2} d^{-1})	0.3±0.1	0.3±0.1	0.3±0.1	0.3±0.1	0	0.1±0.04	0.1±0.04	0.1±0.04	0.4±0.2	0.4±0.2	0.4±0.2	0.4±0.2
^{222}Rn diffusion (Bq m^{-2} d^{-1})	3.1±0.2	3.1±0.2	3.1±0.2	3.1±0.2	2.0±0.1	2.0±0.1	2.0±0.1	2.0±0.1	0.8±0.1	0.8±0.1	0.8±0.1	0.8±0.1

748
749
750
751

752 **Table 5.** The groundwater discharge in Welsby and Mermaid ICOLL and South Welbsy lagoon calculated from the ^{222}Rn mass balance model.

	Welsby ICOLL					South Welsby lagoon					Mermaid ICOLL				
	Summer	Autumn	Winter	Spring	Annual	Summer	Autumn	Winter	Spring	Annual	Summer	Autumn	Winter	Spring	Annual
GW discharge estimates (Daily wind speed averaged over the previous day)															
GW discharge (m^3 d^{-1})	0	3723±2031	4518±2461	3797±2061	3006±1637	0	525±594	128±157	74±99	242±284	163±90	3944±2625	1934±1356	718±358	1697±1107
GW discharge (cm d^{-1})	0	4.2±2.4	5.1±3.0	4.3±2.5	3.4±2.1	0	12.5±10.6	6.4±8.0	3.1±4.2	7.3±8.9	0.4±0.2	5.9±4.1	1.9±1.4	2.1±1.1	2.6±1.7
GW % of lagoon water volume per day	N/A	10.5	12.7	10.7	11.3	N/A	31.3	18.3	10.2	14.9	1.0	14.7	5.5	5.1	6.5
GW discharge estimates (Wind at sampling time)															
GW discharge (m^3 d^{-1})	530 ±200	10146±2925	10543±3064	8361±2416	7395±2151	0	724±402	274±147	116±47	371±254	420±97	9248±5005	2827±1474	3516±2577	4003±1976
GW discharge (cm d^{-1})	0.6±0.3	11.5±4.0	11.9±4.2	9.5±3.3	8.4±3.0	0	17.3±10.2	13.7±7.9	4.8±2.2	11.9±5.3	1.0±0.3	13.7±7.9	2.8±1.6	10.1±4.3	6.9±3.5
GW % of lagoon water volume per day	1.7	28.7	29.8	23.7	20.9	N/A	43.3	39.1	16.0	32.8	2.6	34.3	8.1	25.3	17.5
GW discharge estimates (Wind speed = 50%)															
GW discharge (m^3 d^{-1})	0	1683 ±903	2108±908	1772±755	1373±633	0	262±166	64±38	36±17	121±75	77±42	1966±1278	887±612	364±176	823±527
GW discharge (cm d^{-1})	0	1.9±1.1	2.4±1.1	2.0±0.9	1.6±1.8	0	6.3±4.2	3.2±2.0	1.5±0.8	3.7±2.8	0.2±0.1	2.9±2.0	0.9±0.6	1.1±0.6	1.3±0.8
GW % of lagoon water volume per day	N/A	4.8	6.0	5.0	3.9	N/A	15.7	9.2	5.0	9.9	0.5	7.3	2.5	2.6	3.2

753

754 **Table 6.** Groundwater role in lake Hydrology from previous studies. Table updated from
755 Perkins et al. (2015). ICOLLs are more groundwater-dominated than most other lakes.

System name (location)	Ave. depth (m)	Ave. surface area (m^2)	Volume (m^3)	Shoreline length (m)	GW flux (cm d^{-1})	Rainfall (cm d^{-1})	Lake volume replaced in a day (%)	GW:Rain ratio over an annual cycle	Shoreline length: lake volume	Authors
Welsby ICOLL (Australia)	0.4	88,386	36,459	1680	4.00	0.24	11.35	16.83	0.046	This study (2015)
South Welsby Lagoon (Australia)	0.3	3,137	785	800	5.40	0.24	14.9	16.74	1.019	This study (2015)
Mermaid ICOLL (Australia)	0.4	67,429	154,344	3560	3.40	0.24	6.50	14.33	0.023	This study (2015)
Sale Common Wetland (Australia)	2.0	3 × 10^6	6 × 10^6	10500	0.40	0.16	0.20	2.50	0.002	Gilfedder et al., (2015)
Lake Ainsworth (Australia)	4.4	1.25 ×10^5	550 × 10^3	1690	0.67	0.49	0.37	1.37	0.003	Perkins et al., (2015)
Little lagoon (AL, USA)	1.5	10.5× 10^6	1575× 10^4	27555	1.45	0.45	0.01	3.22	0.002	Su et al., (2015)
Newmans lake (Florida, USA)	1.5	2.98 × 10^7	44,700 × 10^3	19500	0.50	0.36	0.002	1.39	0.000	Dimova et al., (2013)
Butler lake (Florida, USA)	4.2	6.38 × 10^6	26,796 × 10^3	17000	0.30	0.36	0.56	0.83	0.001	Dimova et al., (2013)
Clear lake (Florida, USA)	3.7	1.45 × 10^6	5,365× 10^3	4500	0.30	0.36	0.36	0.83	0.001	Dimova et al., (2013)
Haines lake (Florida, USA)	2.1	2.91 × 10^6	6,111× 10^3	7100	1.00	0.36	0.48	2.78	0.001	Dimova et al., (2013)
Shipp lake (Florida, USA)	1.5	1.12 × 10^6	1,680× 10^3	3770	0.10	0.36	0.07	0.28	0.002	Dimova et al., (2013)
Josephine lake (Florida, USA)	1.8	5.8 × 10^6	10,440× 10^3	14370	1.60	0.36	0.43	4.44	0.001	Dimova et al., (2013)
Marina lagoon (Eygpt)	3.5	4× 10^6	14× 10^6	22000	6.00	0.13	0.02	46.2	0.002	El-Gamal et al. (2012)
Round lake (Florida, USA)	2.1	34,900	73,290	700	0.0	0.36	-	-	0.009	Dimova & Burnett (2011)
SM8 (Canada)	0.9	1.91 × 10^6	1,719× 10^3	6700	0.05	0.12	0.56	0.42	0.004	Schmidt et al., (2010)
Lake Ammelshainer (Germany)	10.0	5.3 × 10^5	5.6 × 10^5	3265	18.6	0.16	17.61	116	0.006	Schmidt et al., (2009)
Mangueira (Brazil)	4.5	9 × 10^8	4,050 × 10^6	216264	0.60	0.34	0.01	1.76	0.0001	Santos et al., (2008)
Willersinnweiher (Germany)	8.0	1.45 × 10^5	1,160× 10^3	2200	0.40	0.18	0.05	2.22	0.002	Kluge et al., (2007)

756

757

Figure legends

Figure 1. Map of the study site. Red points indicate location of groundwater wells. The grey circle on Australia map indicates the study area.

Figure 2. Conceptual model of ^{222}Rn mass balance approach used to quantify groundwater discharge into the ICOLLs. All relevant sinks and sources of ^{222}Rn were quantified and the missing ^{222}Rn was assigned to groundwater discharge.

Figure 3. Contour maps of ^{222}Rn concentrations and salinity for Welsby ICOLL during seasonal field measurements. *Note the different colour coding to highlight spatial trends in each season.*

Figure 4. Contour maps of ^{222}Rn concentrations and salinity for South Welsby Lagoon during seasonal field measurements. Dark parts indicate areas with no data due to very shallow water. *Note the different colour coding to highlight spatial trends in each season.*

Figure 5. Contour maps of ^{222}Rn concentrations and salinity for Mermaid ICOLL during seasonal field measurements. Dark parts indicate areas with no data due to very shallow water. *Note the different colour coding to highlight spatial trends in each season.*

Figure 6. Shoreline length versus percentage of lake volume replaced in a day. Lake Ammelshainer in Schmidt et al. (2009) study has a very high lake volume replacement in a day and is considered an outlier.

Figure 7. A conceptual model describing groundwater discharge processes in ICOLLs. The upper panel demonstrates conventional salt fingers at the sediment-water interface when groundwater levels are low while the lower panel illustrates fresh groundwater discharge and saline groundwater forcing process when groundwater levels are higher.

Figure 8. Groundwater discharge versus salinity plots. South Welsby is not shown here as salinity did not vary in the wetland.

792 **Figure 1**

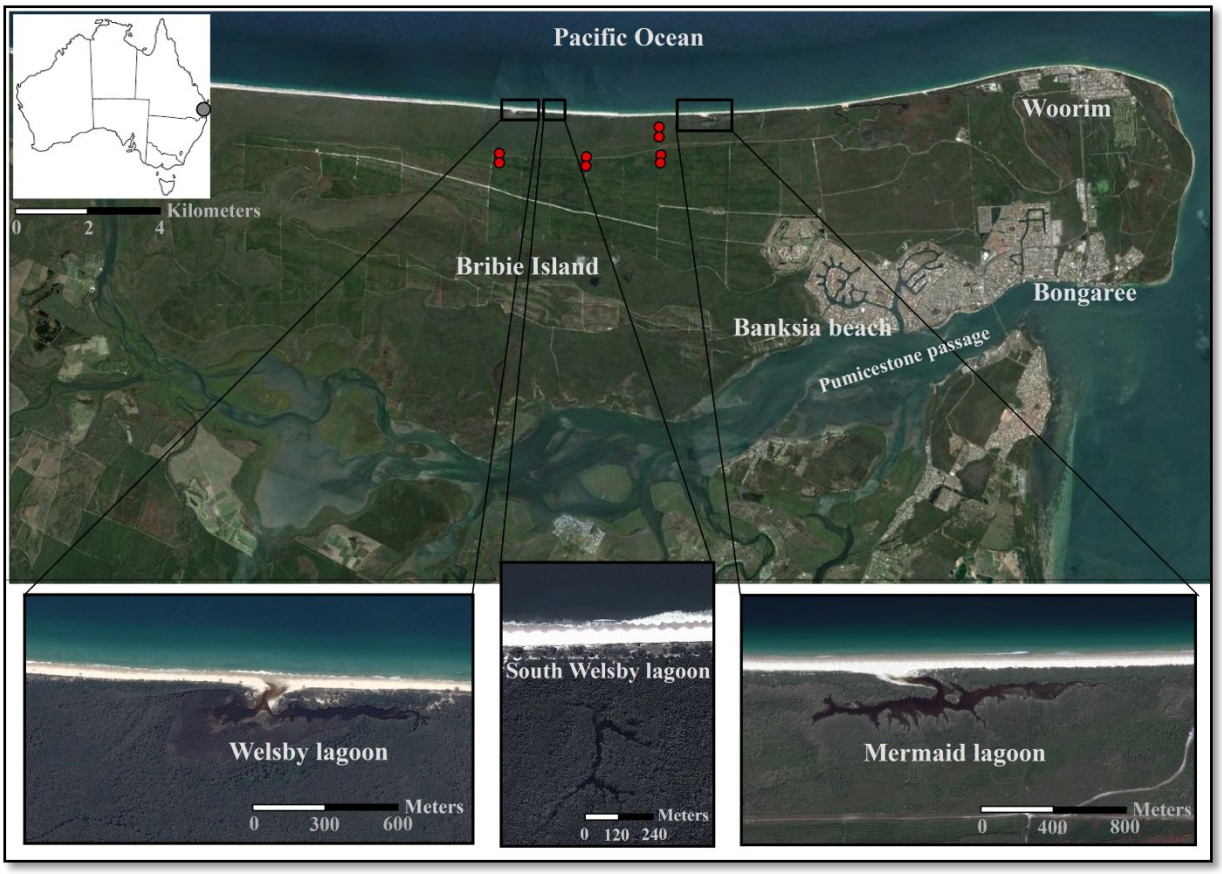

793

794

Figure 2

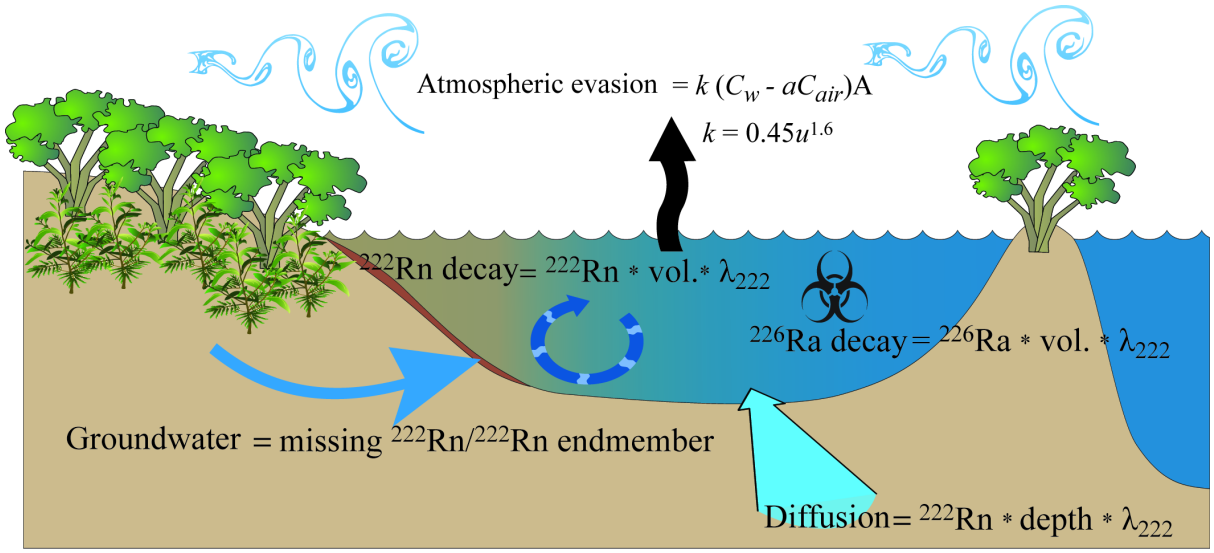
Atmospheric evasion $= k\,(C_w - aC_{air})A$
$k = 0.45u^{1.6}$
^{222}Rn decay= ^{222}Rn * vol.* λ_{222}
^{226}Ra decay= ^{226}Ra * vol. * λ_{222}
Groundwater = missing ^{222}Rn/^{222}Rn endmember
Diffusion= ^{222}Rn * depth * λ_{222}

799 **Figure 3**

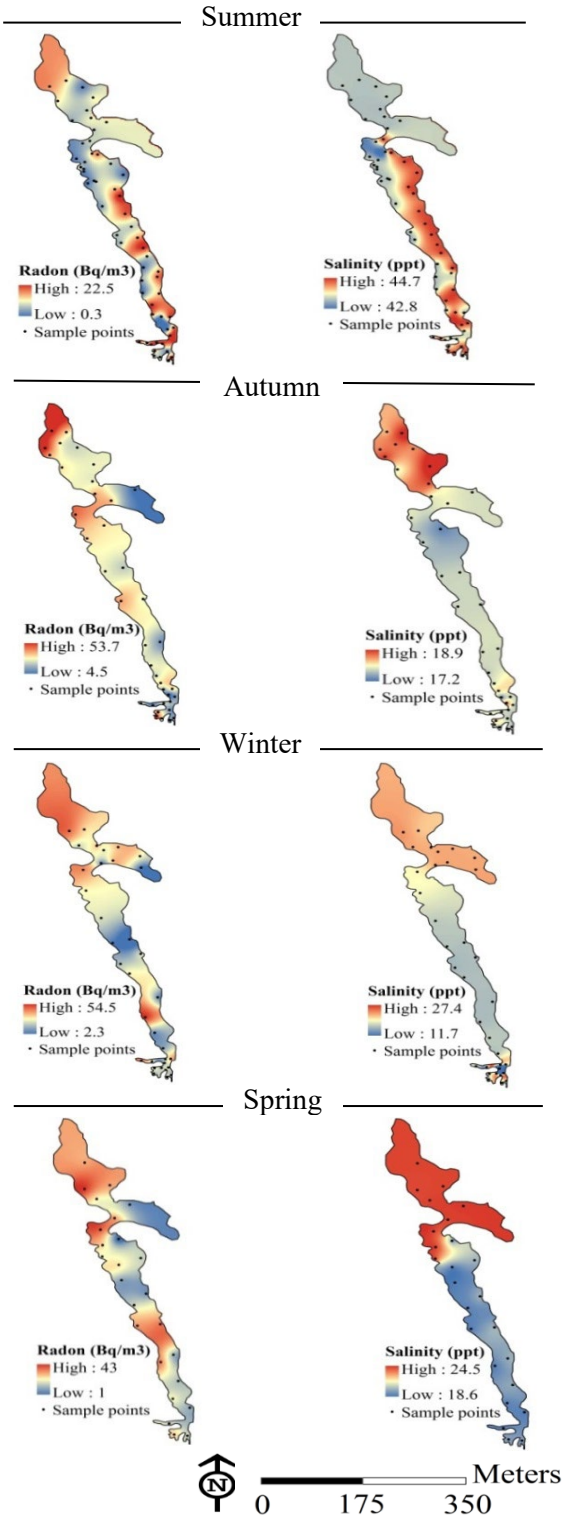

800

801

802 **Figure 4**

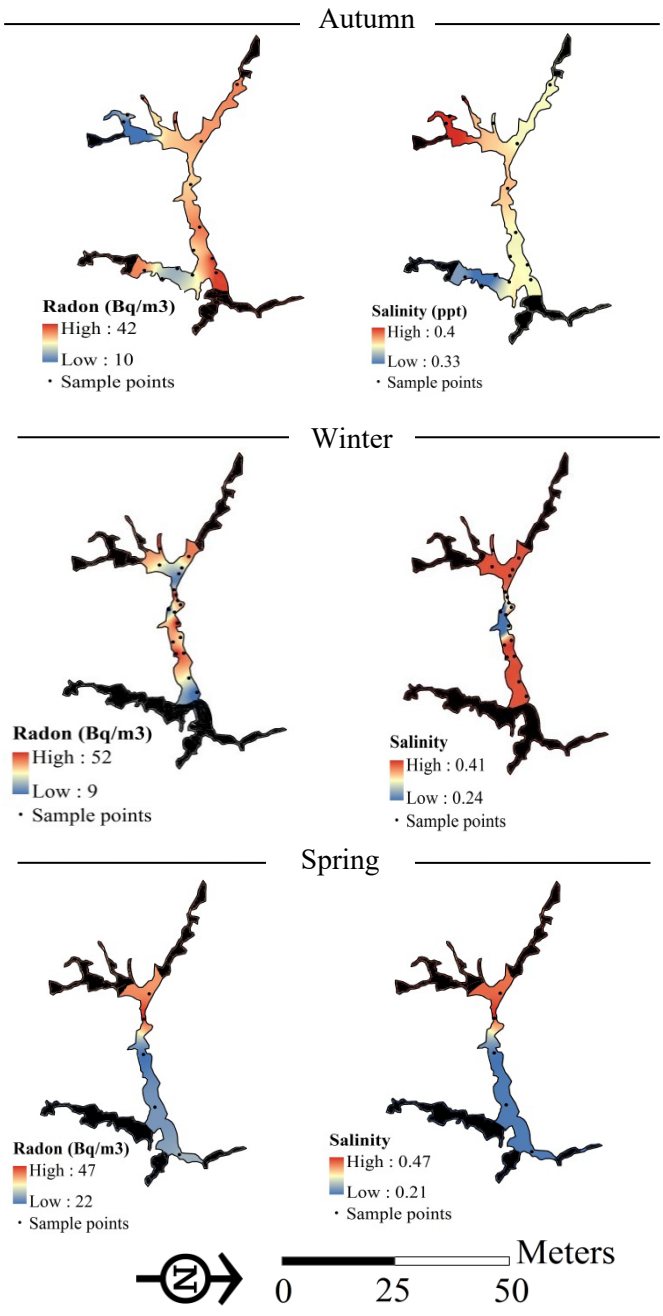

803

804

805 **Figure 5**

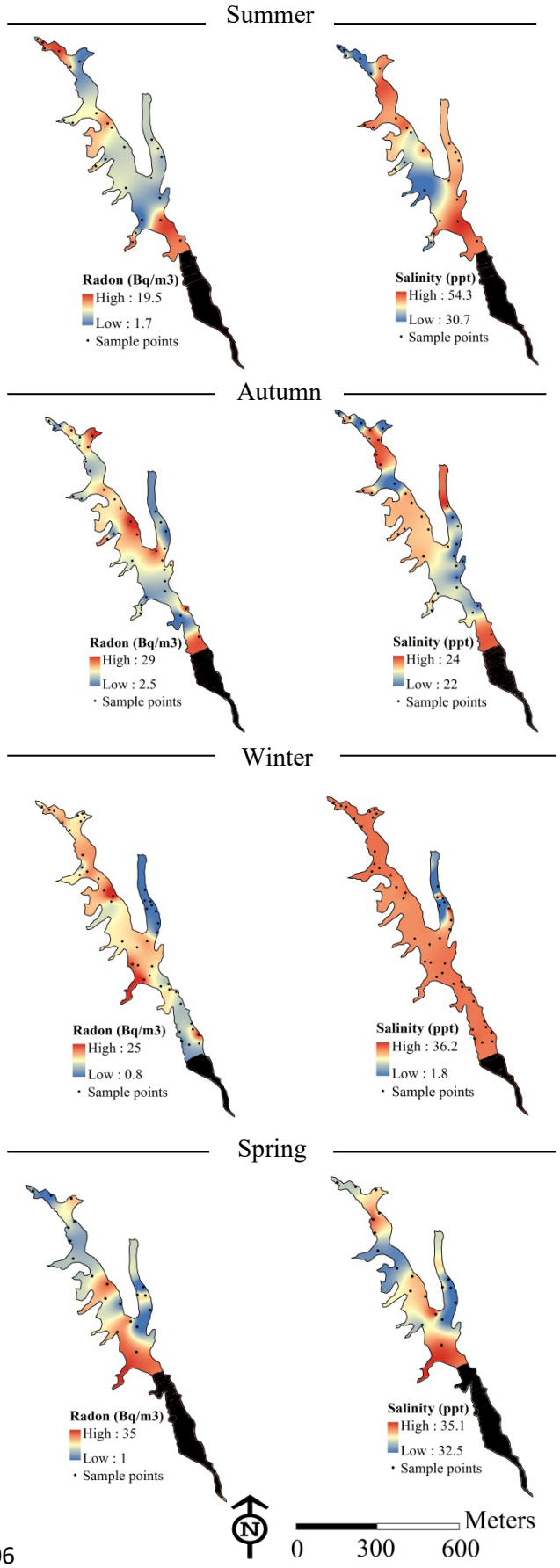

806